



IDENTIFICATION OF INSTANTANEOUS STIFFNESS AND MODAL DAMPING RATIO IN A REINFORCED CONCRETE BRIDGE COLUMN SUBJECTED TO SEISMIC LOADS

C.A. Gaviria⁽¹⁾, L.A. Montejo⁽²⁾

⁽¹⁾ Assistant Professor, Civil Engineering Program, Universidad Militar Nueva Granada, UMNG, Bogotá, Colombia, carlos.gaviria@unimilitar.edu.co (Researcher, Civil Engineering Program, Universidad de la Costa, Colombia)

⁽²⁾ Associate professor, Dept. of Engineering Science and Materials, University of Puerto Rico at Mayaguez, luis.montejo@upr.edu

Abstract

An iterative unscented Kalman filter (UKF) combined with a piece-wise nonlinear model is proposed to estimate instantaneous stiffness and damping ratios during the response of the structure to the earthquake motion. The methodology is evaluated based on simulated and experimental data collected on a real-scale RC column test performed at the NEES Large High Performance Outdoor Shake Table. Results show that the identified instantaneous stiffness and damping ratios are in close agreement with the actual stiffness and total hysteretic damping exhibited by the structure, respectively. Moreover, it was found that the maximum values of damping and minimum values of stiffness reached by the structure during its dynamic response are better indicator of damage than post-event identified properties.

Keywords: Health Monitoring; Kalman Filter; System Identification; Reinforced Concrete; Bridge

1. Introduction

Identification of dynamic structural properties has been a fundamental aspect of vibration based health monitoring of civil structures. Nevertheless, the use of changes in the natural frequency and damping ratios as pointers of the level of damage induced in RC structures is debatable as they tend to saturate at large levels of inelastic demand and their identification during forced dynamic responses can be troublesome [1-3]. Therefore, direct identification of peak displacements, and shifts in stiffness and damping are desirable as they are robust indicators of the level of damage induced in the structure.

The viability of using numerical models to validate damage detection methodologies has been evaluated in the past (e.g. [4-5]). Using detailed numerical models that can closely replicate damage episodes allows for a comprehensive evaluation of SHM methodologies since structural parameters can be retrieved for a wide range of inelastic demands. Moreover, Kalman based approaches can engage the measured dynamic response and a numerical model of the structure to identify real time variations of the structural parameters. Over the last years, an optimal recursive estimator robust to noise contaminated signals called the unscented Kalman filter (UKF) have been studied for identification of civil structures (e.g. [6-8]). The UKF is employed more than other Kalman filter approaches as it is more adaptable to track changes since it does not require the partial derivatives of the state vector or Jacobian [6-9]. Nevertheless, the UKF approach is not intended to track sudden variations of the model parameters that could be caused by abrupt damage of one or more structural members [7]. Mariani and Ghisi [6] identified variations in stiffness using the UKF and a five parameters model of elastic damage on the simulated response of a SDOF system under constant and linear forces. They found that this approach can identify stiffness degradation due to damage growth. Bisht and Singh [7] proposed an approach to adjust the state covariance matrix in the UKF for the tracking of sudden changes in stiffness values. Simulated data of two and six degree of freedom (DOF) models with abrupt stiffness reduction (linear damage) and subjected to different earthquake motions were examined. The outcomes indicate that the proposed method is able to track single and multiple stiffness changes at different time instances and at different structural elements. However, a threshold value (β parameter) need to be tuned by the user for a particular structure and, large levels of noise can introduce false changes in the structural properties. Chaabane et al. [8] used an iterated square-root central difference Kalman particle filter method (ISRCDKF-PF) for two different scenarios, showing that the ISRCDKF-PF provide better accuracy and convergence than several particular filter (PF) and UKF schemes when abrupt changes in estimated states take place.

In the aforementioned research, several UKF based approaches have been proposed to detect sudden strong nonlinear variation of the structural parameters that could occur in RC structures. However, a calibration and validation of these approaches performed based on experimental results from full scale shake table tests or detailed nonlinear numerical models of a RC structures exhibiting highly nonlinear behavior is missed. This article presents an alternative UKF based scheme to estimate instantaneous stiffness and dissipative properties of RC structures undergoing damaging processes while subjected to earthquake loads. A numerical study is conducted using simulated data from a fiber-based distributed-plasticity finite element model calibrated to closely replicate the nonlinear dynamic response of a full scale reinforced concrete bridge column [4] tested on the NEES-UCSD Large High Performance Outdoor Shake Table [10]. The data was contaminated with different levels of noise to examine the capabilities of the proposed approach to track stiffness and damping ratios in realistic scenarios. Additional validation was performed using the actual data registered during the shake table tests.

2. The implemented UKF and numerical model of the structure

The UKF is a recursive statistical approach that generates a set of possible responses and parameters of the structures at each time step. In this study, these responses are estimated using: a) the properties and initial condition of the structure, b) the current acceleration at the base, c) a model of the behavior of the structure, d)

the covariance matrix of all parameters and responses in the previous step of analysis and, e) the acceleration at each floor. At the start point of analysis, the initial properties of the structure can be estimated using, for example, a set of recorded ambient vibration of the structure. The acceleration at base and at each floor can be measured within a structural health monitoring (SHM) scheme during a seismic event. A non-parametric representation of the nonlinearity based on the equation of motion of a damped system is adopted to represent the nonlinear dynamic response of the system:

$$[M]\{\ddot{u}\} + [C]\{\dot{u}\} + [K]\{u\} = -[M]\{r\}\{\ddot{u}_g\} \quad (1)$$

where M is the mass matrix (constant), C and K are the damping and stiffness matrices that are updated each time step, r is the influence coefficient vector, \ddot{u}_g is the input acceleration at the base and, u , \dot{u} and \ddot{u} are the displacement, velocity and acceleration response vectors correspondingly. For simplification of the formulation, the rotational DOFs are not considered explicitly, thus the complete behavior of the system is condensed in the translational DOF. The recursive solution of the equation of motion is accomplished by the average acceleration method that provides a direct integration of Eq. (1) and calculates de displacement and its derivatives. As a result, the responses monitored in the implemented method are the displacement, velocity and acceleration. The time-variant parameters of the structure are the stiffness and modal damping ratios.

The UKF generates a set of $2L + 1$ possible responses and parameters of the structure in the previous time interval $i-1$ and, each response is stored as a column vector in the matrix $\hat{x}_{i-1,n}$ (see Eq. (2)). L is the number of responses to be estimated and $\lambda = 3 - L$ is a characteristic scaling parameter [11]. This set of possible values are evaluated in the Eq. (1) to calculate a set of possible responses $\hat{x}_{i,n}$ at the current time step i .

$$\begin{aligned} \hat{x}_{i-1,0} &= x_{i-1} \\ \hat{x}_{i-1,n} &= x_{i-1} + \sqrt{L + \lambda} * (\sqrt{P_{i-1}})_n \quad n = 1, 2, \dots, L \\ \hat{x}_{i-1,n} &= x_{i-1} - \sqrt{L + \lambda} * (\sqrt{P_{i-1}})_{n-L} \quad n = L + 1, \dots, 2L \end{aligned} \quad (2)$$

Eq. (2) shows that the spread of probable responses of the structures is fixed by the time-variant covariance matrix of the system P_{i-1} . This covariance matrix incorporates the connection between all parameters and responses considered in the structural model of the structure. For the implemented UKF, the P_i matrix at time step i is computed in three steps (Eqs. (3) - (5)). First, the gross covariance matrix \hat{P}_i is computed with the set of possible responses $\hat{x}_{i,n}$ (Eq. (3)). Where $\hat{x}_i^{(m)}$ is the mean probable response, $W_n^{(c)}$ is a vector with the weights for the covariance and, Q is typically a constant covariance matrix that collect the noise (i.e. misleading values) arising during the recursive solution of the equation of motion due to propagation of the noise embedded in the recorded acceleration at base. As is proposed in the next section, a time-variant Q matrix can be used for a fine tuned of the covariance matrix of the system and capture the strong nonlinear behavior in the stiffness and damping ratios.

Secondly, a covariance matrix of the estimated accelerations $P_{\hat{y}\hat{y}}$ (i.e. the covariance of the variables directly sensed in the structure) is computed (Eq. (4)) using a set of estimated accelerations $\hat{y}_{i,n}$, the mean estimated acceleration $\hat{y}_i^{(m)}$ and, the covariance matrix of the noise in the measured accelerations R . The constant matrix R is diagonal and it is composed by the square of the root mean square (RMS) value of the estimated noise in each acceleration monitored. This matrix allows incorporating an additional dispersion in the estimated measured responses of the structure that is equal to the level of noise in the actual measured accelerations. The instantaneous covariance matrix of the system P_i is estimated by combination of the matrices \hat{P}_i and $P_{\hat{y}\hat{y}}$ with the Kalman gain matrix K_i (Eq. (5)).

$$\hat{P}_i = \sum_{n=0}^{2L} W_n^{(c)} \left(\hat{x}_i^{(m)} - \hat{x}_{i,n} \right) \left(\hat{x}_i^{(m)} - \hat{x}_{i,n} \right)^T + Q \quad (3)$$

$$P_{\hat{y}\hat{y}} = \sum_{n=0}^{2L} W_n^{(c)} \left(\hat{y}_i^{(m)} - \hat{y}_{i,n} \right) \left(\hat{y}_i^{(m)} - \hat{y}_{i,n} \right)^T + R \quad (4)$$

$$P_i = \hat{P}_i - K_i P_{\hat{y}\hat{y}} (K_i)^T \quad (5)$$

Finally, the optimal response and parameters of the structure x_i are estimated by using the measured accelerations in the system z_i (see Eq. (6)). Others parameters employed by the UKF algorithm were updated based on reported values of recent studies on civil infrastructure (e.g. [9]). The scaling parameters used to fine tune the high order statistics moments α and k were fixed to 10^{-3} and 0 respectively [9]. The initial covariance matrix P_0 is a diagonal matrix with a value of 10^{-6} in all diagonal elements [11]. A more detailed description of the UKF algorithm is presented in Brown and Hwang [12].

$$x_i = \hat{x}_i^{(m)} + K_i \left(z_i - \hat{y}_i^{(m)} \right) \quad (6)$$

3. Improving the UKF algorithm for RC structures subjected to seismic loads

A reported limitation of the implemented UKF approaches is to keep an adequate spread of the possible responses of the structure to capture the high variation of the model parameters due to damaging events [6, 8]. The scatter of the estimated responses is conducted by the covariance matrix P as discussed in the previous section (Eq. (2)). Taking into account that the matrix Q influences directly the covariance matrix (Eq. (3)) a rational definition of a time-variant Q matrix is proposed.

Typically, a diagonal Q matrix fixed to a small entry of 10^{-25} is used [6]. Nevertheless, considering that the instantaneous estimated values are collected in a vector x_i and it is composed by the response and parameters of the structure, the covariance matrix Q is split in two diagonal matrices Q_s and Q_b . The Q_s matrix represents the propagation of the noise embedded in the input of the model (i.e. the recorded acceleration at the base) that is reflected in the output (i.e. the response of the system). The inaccuracy in the evolution of the stiffness and damping ratios are collected in the covariance of noise matrix Q_b . The matrices Q_s and Q_b at time t_i are defined as:

$$[Q_s]_i = \text{diag} \left[\gamma_s * \left(\text{RMSn}_{\ddot{x}_g} / \ddot{u}_{max} \right) * \left\{ u_{max}^T \quad \dot{u}_{max}^T \quad \ddot{u}_{max}^T \right\} \right]^2 \quad (7)$$

$$[Q_b]_i = \text{diag} \left[\gamma_b * \left\{ k_{max}^T \quad \xi_{max}^T \right\} \right]^2 \quad (8)$$

where u_{max} , \dot{u}_{max} and \ddot{u}_{max} are the estimated maximum displacement, velocity and acceleration (relative to the base) and, k_{max} and ξ_{max} are the maximum stiffness and damping ratio during the analyzed seismic event. $\text{RMSn}_{\ddot{x}_g}$ is the RMS of noise in the acceleration at the base. The term $\text{RMSn}_{\ddot{x}_g} / \ddot{u}_{max}$ is a dimensionless factor that generalizes Eq. (7) for different levels of noise. γ_s and γ_b are constants for tuning the minimum deviation needed to capture the high variation of the model parameters. Values of $\gamma_s = 0.01$ and $\gamma_b = 0.001$ were found appropriate by the authors for a large range of input intensities and inelastic demands after numerous analyses of simulated response of SDOF and MDOF shear building models subjected to a set of seismic records. The maximum values of the responses and parameters in the structure for each particular earthquake excitation are estimated with an iterative UKF scheme:

- In the first iteration a low level of noise (RMS = 0.001g) is used to estimate the optimal Q matrix (Eqs. (7)-(8)). If after 25 iterations the maximum responses and variations of the parameter do not converge to stable values, the RMS of the noise is increase in 0.001g. This variation in the level of noise provides an additional gap between the measured vibrations and the response predicted by the filter that increases the stability of the proposed UKF scheme.

- The values of u_{max} , \dot{u}_{max} , \ddot{u}_{max} , k_{max} and ξ_{max} are set to zero at the first iteration of UKF analysis. These maximum values are recalculated at the end of the each iterative UKF analysis from their estimated response and parameters. These updated values are then used to compute the Q_i matrix for the next iteration.
- The calculated Q_i matrix is amplified or reduced by a smoothed envelope of the input accelerations (i.e. an instantaneous Q_i matrix is used). Thus, the values in the Q matrix may appropriately increase in a particular time instant so that the scatter of probable responses of the structures can be enough to reach the actual nonlinear measured response of the structure. Otherwise, Q matrix is reduced. This procedure minimizes the bias estimation of the parameters induced after the strong motion part of the excitation fades away and the structure oscillates at low amplitudes boosting the detrimental effect of noise.
- The convergence of iterative UKF process is reached when the difference of the parameters estimated in the last 3 iterations falls below 5%.

Fig. 1 shows examples of displacements, frequencies and damping ratios time histories estimated using the proposed Q matrix and the classical Q matrix fixed to a small entry of 10^{-25} [6]. Two cases are presented that correspond to low (EQ1 - no rebar yield) and high (EQ7 - rebar buckling) inelastic demand (further details on the structure and the data employed are presented in the next sections). It is seen that the estimates obtained with the proposed Q matrix are in closer agreement with the actual values than the ones arising from the use of traditional fixed-low valued Q , i.e. the conventional definition of Q may be not sufficient to capture the high variation of the model parameters expected on severe earthquakes. A more detailed and comprehensive description analyses performed and the results obtained are presented in the following sections.

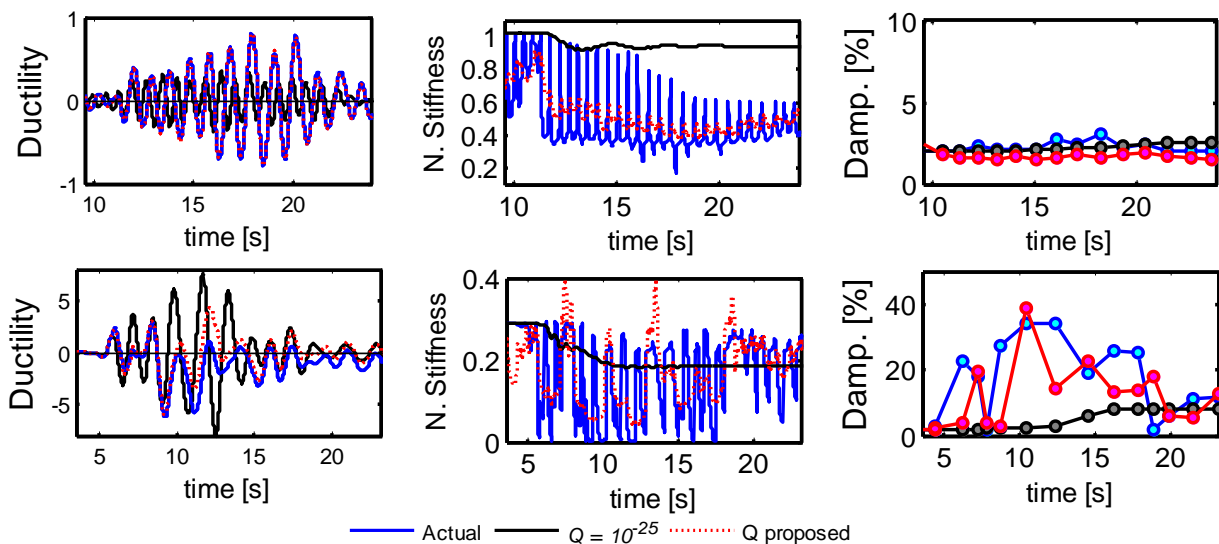


Fig. 1 – Comparison of UKF results using traditional fixed-low valued and the proposed Q for low (top figures) and large inelastic demand (bottom figure) scenarios

4. The circular RC bridge column

Validation of the proposed UKF method is accomplished using experimental and simulated data from a series of full-scale circular RC bridge column shaking table tests performed at the NEES-UCSD Large High Performance Outdoor Shake Table (Fig. 2). The column specimen has a diameter of 1.22 m with a cantilever length of 7.32 m, reinforced by 18 longitudinal bars #11 (i.e. longitudinal reinforcement ratio of 1.5%) and #5 hoops at 0.152 m. Also, a reinforced concrete block with a weight of 2245kN was built at the top. The column was exposed to a sequential load of ten earthquake ground motions (EQ) with different levels of intensity. Due to space constraints, only the results for no rebar yield / concrete spalling (EQ1), first significant inelastic excursion (EQ3), rebar buckling (EQ7), and rebar fracture (EQ8) are presented. All experimental data was obtained from the NEES Project Warehouse repository. Further details on the specimen and test setup are available elsewhere [4,10].

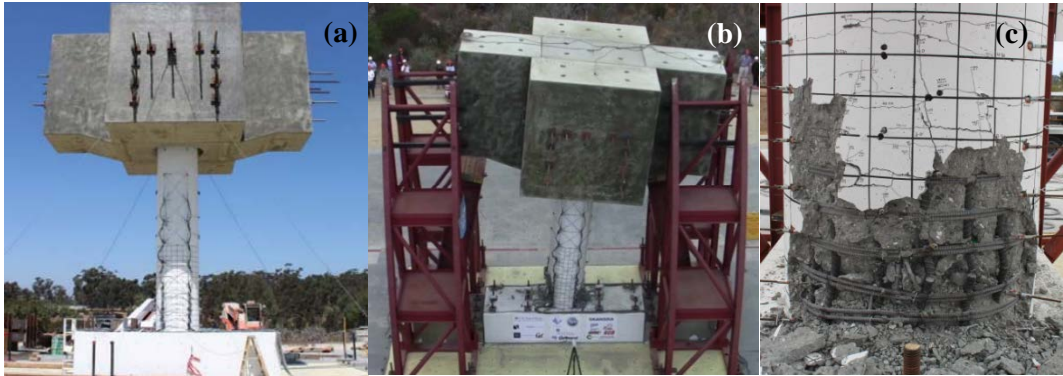


Fig. 2 – Full-scale RC bridge column test (photos taken from: <https://nees.org/warehouse/project/987/>). (a) Pre-test Column, (b) Post-test Column and (c) Column base east face during EQ10.

Simulated data from a fiber-based distributed-plasticity finite element model of the column calibrated to closely replicate the nonlinear dynamic response of the full scale reinforced concrete bridge column test [4] is used first. This data allows to compare the structural parameters (e.g. stiffness) of the numerical model and the estimated values by the proposed UKF scheme for a wide range of inelastic demands. The column section was represented by unidirectional fibers and constitutive-material relationships were specified for each kind of fiber (unconfined concrete, unconfined concrete and reinforcing steel). Other information about the numerical model can be found elsewhere [4]. The methodology is also applied to the actual experimental data. To reduce the detrimental effect of noise, a low-pass filter with a cutoff frequency of 25Hz is applied to the accelerations at the top and bottom of the column before they are used in the identification scheme.

5. Results using simulated data

In this section, the results of the implementation of the proposed UKF approach are presented and discussed. In addition to the ideal case of no noise contamination, a low, intermediate and very high noise levels (i.e. levels of noise with root mean square (RMS) values of 0.001g, 0.005g and 0.01g) were added to the simulated response of the structure. The displacements estimated by the UKF in the form of time histories of ductility demand (yield displacement was 0.093 m) are presented in Figs 3(b) – 6(b). It is seen that the methodology is robust to the presence of noise, i.e. the displacement estimates for the cases with and without noise are very similar and close to the actual response. While the residual displacements that appear at increasing seismic intensities are not captured due to the non-hysteretic nature of the model used, the peak displacements are successfully captured over the wide range of inelastic demands examined.

Figs. 3(c)-6(c) shows the results obtained for the change in stiffness expressed as a fraction of its initial value of the pristine structure ($k_0 = 1.8663 \text{ kN/m}$). To allow comparisons and since the structure is highly dominated by the first mode, for the simulation results an equivalent lateral stiffness was defined based on the first natural frequency values retrieved from the model. Notice that the estimated stiffness shifts can be seen as a smoothed version of the actual behavior.

Total equivalent damping ratios from the numerical model results are calculated as the specified elastic damping ratio plus the hysteretic damping (ξ_h) estimated using the Jacobsen's approach without any corrections factors e.g. [13, 14]:

$$\xi_h = \frac{2 A_1}{\pi A_2} \quad (9)$$

where A_1 is the area inside each hysteretic loop and A_2 is the area of a rigid, perfectly plastic member with the same maximum strength and the same maximum displacement in each direction as the actual member. Since the areas A_1 and A_2 can be computed only on a full loop basis, the calculated damping ratios can be seen as average values over the loop and are assigned to the half-time duration of the loop. For comparison purposes,

the instantaneous values of damping ratios estimated by the UKF approach are averaged in the same full loop of displacement of the numerical model result. The results obtained are presented in Figs. 3(d) to 6(d). It is seen that the total equivalent damping calculated from the numerical model has the same shape of the average damping ratios estimated by the UKF approach. As expected, for low levels of excitation where the structure remains mostly on the elastic range (i.e. EQ1), the hysteretic damping is small and the total damping remains mostly constant at the elastic damping value. As one moves towards larger levels of excitation (i.e. EQs 3, 7 and 8) the hysteretic damping contribution becomes dominant during the strong motion part of the response due to a number of significant inelastic excursions.

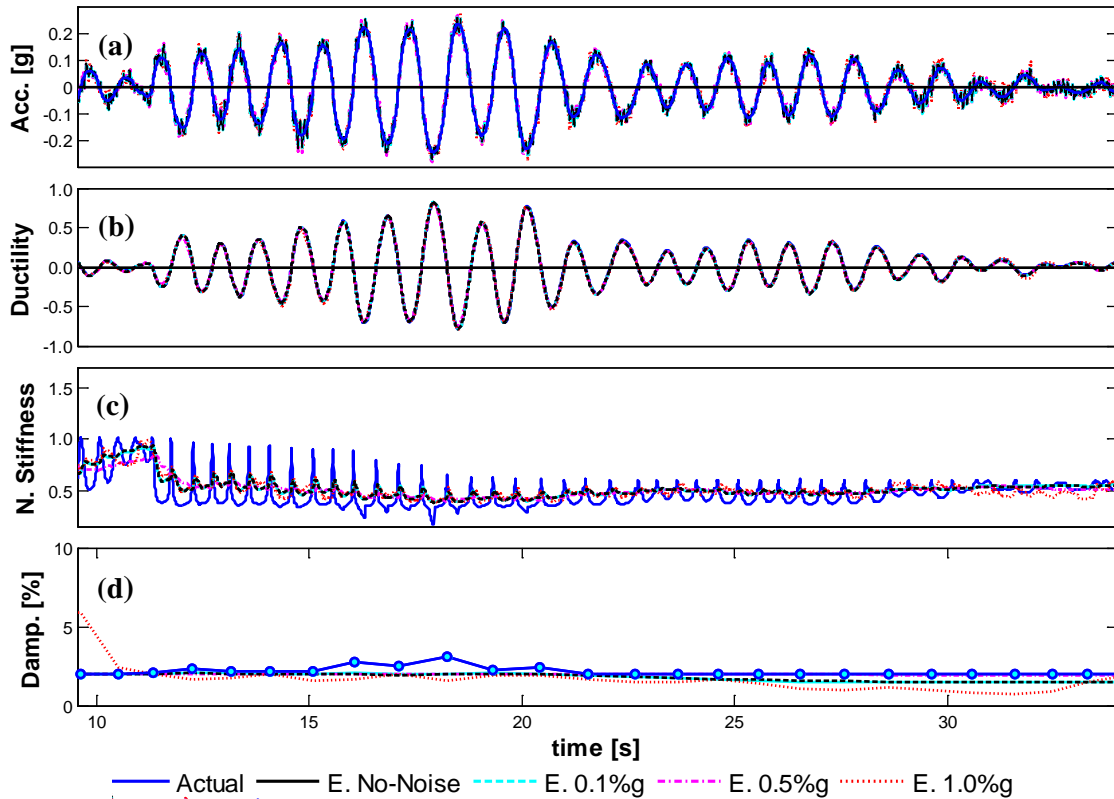


Fig. 3 – Estimated acceleration, displacement, stiffness and damping ratio time histories when the column is subjected to EQ1 (linear range).

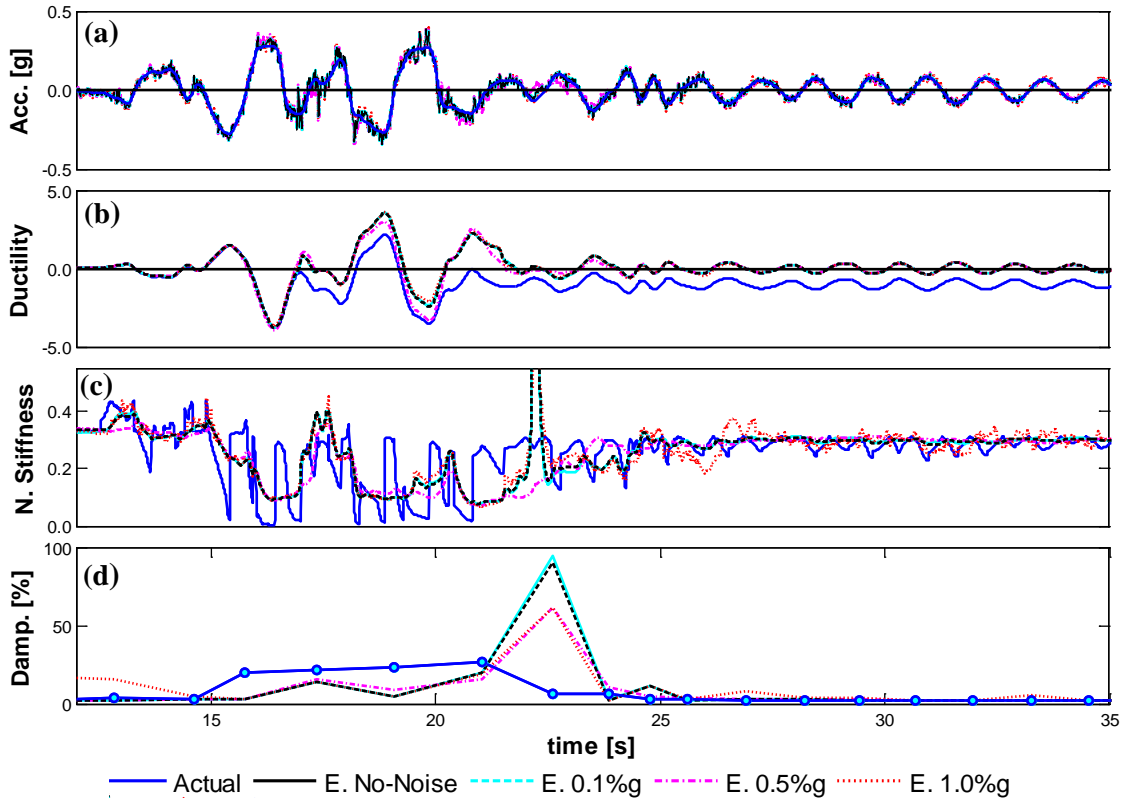


Fig. 4 – Estimated acceleration, displacement, stiffness and damping ratio time histories when the column is subjected to EQ3 (first significant inelastic excursion)

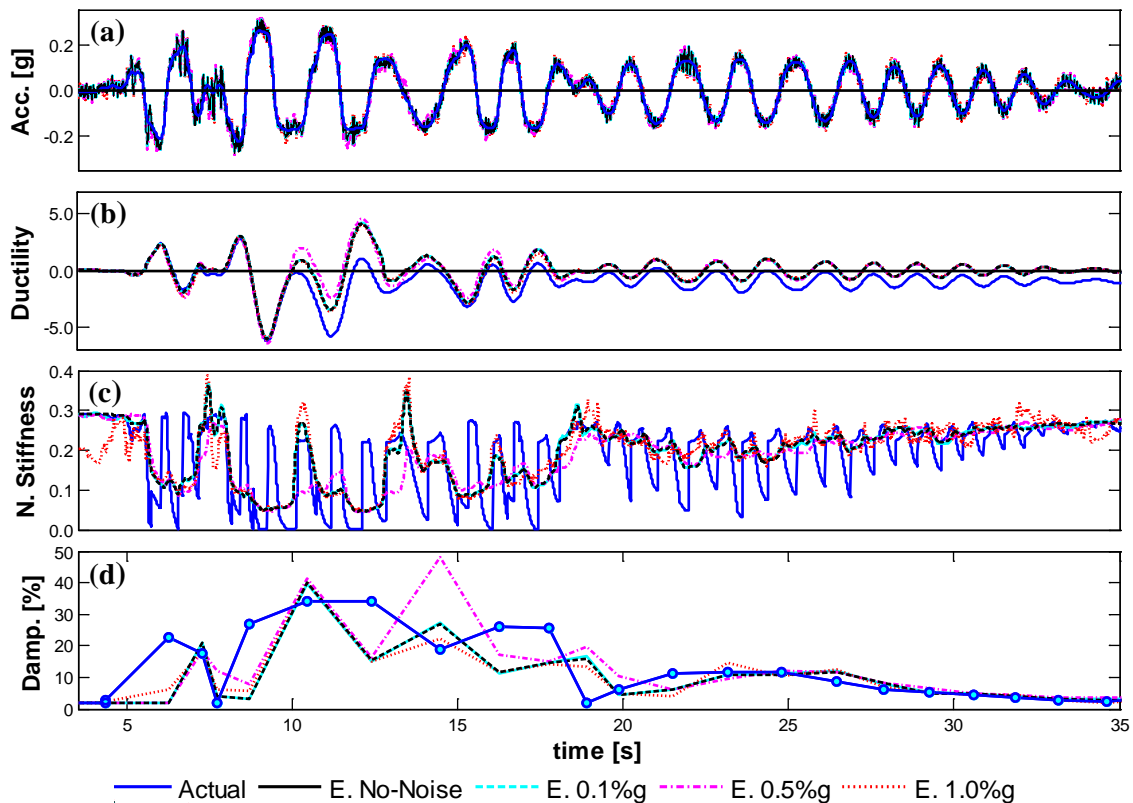


Fig. 5 – Estimated acceleration, displacement, stiffness and damping ratio time histories when the column is subjected to EQ7 (rebar buckling)

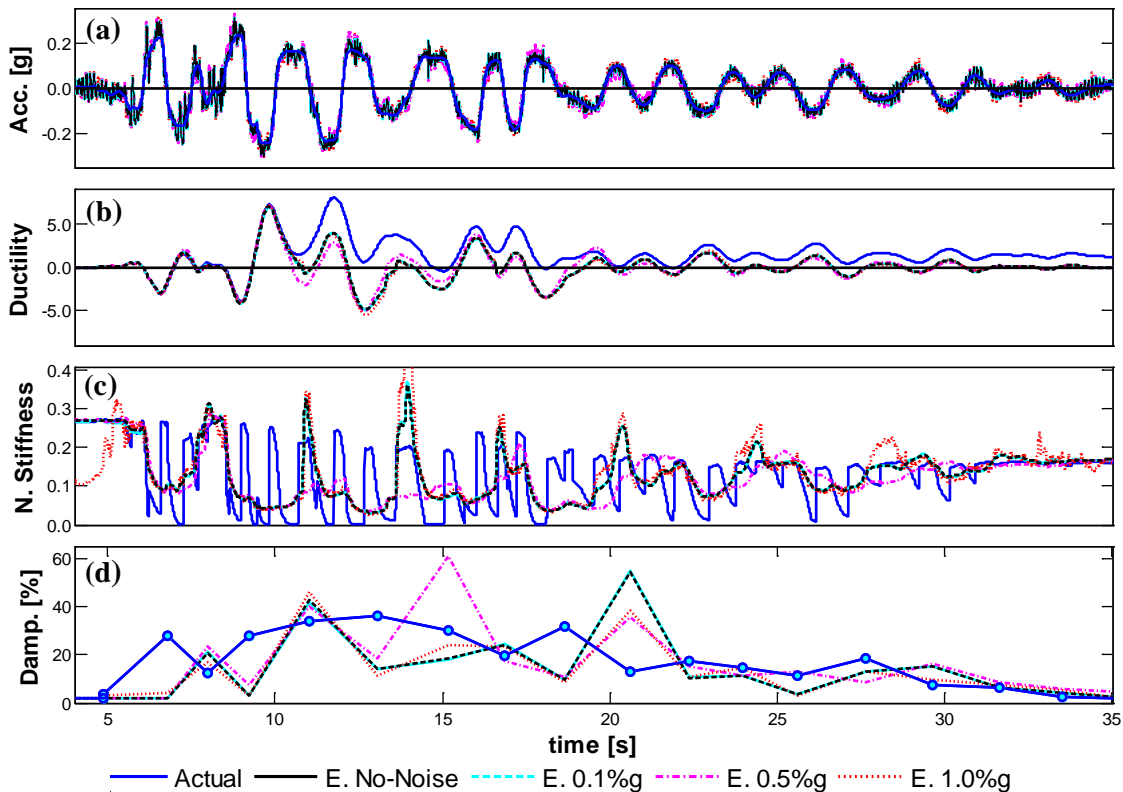


Fig. 6 – Estimated acceleration, displacement, stiffness and damping ratio time histories when the column is subjected to EQ8 (rebar fracture)

The capacity of the UKF scheme for tracking the dynamic/structural properties of the system was discussed in the previous paragraphs. The results for all earthquake scenarios and contaminated by all level of noises are consolidated here to investigate the feasibility of using these parameters as indicators of damage. Fig.7 shows the estimated normalized minimum values of the stiffness (left) and the stiffness at the end of each record (right) for all noise levels versus the actual ductility demand reached by the column, an exponential regression using the estimated UKF values without noise is also included. It is seen that the minimum value of stiffness is less affected by the noise level than the stiffness at the end of the earthquake (i.e. the estimated minimum value of stiffness for all levels of noise has a low dispersion). Moreover, the minimum value of stiffness is more sensible to the induced inelastic demand in the structure and correlates better with the ductility than the stiffness after the record.

Fig.8 summarizes the maximum values of damping ratio achieved during the seismic excitation and the damping ratios at the end and, a linear regression using the estimated UKF values without noise. As for the stiffness results, it is seen that the maximum damping value correlates better and is more sensible to the induced inelastic demand in the structure than the damping ratio after the record.

6. Results using experimental data

The proposed UKF approach is now applied to the actual experimental data from the full scale column shake table tests. The acceleration responses at the top of the column as well as the shake table accelerations were measured during this test and are used in the analysis. The noise RMS is calculated using the first 8 seconds of the measured data when the shaking table was static; the values obtained were 0.0029g and 0.0012g (i.e. low to intermediate levels of noise) for the accelerations at the base and top, respectively. The results obtained from the proposed UKF scheme are presented in Fig. 9. The estimated displacements are compared with the experimental displacements measured with a string potentiometer located at top of the column. Estimated stiffness are compared with the initial and final stiffness of the column computed based on the initial and final natural frequency values identified via Fourier spectra of the column acceleration response to low amplitude white noise

excitations applied between earthquakes [15]. The hysteretic damping contribution to the total equivalent (TE) damping ratio is calculated from the areas of the force-displacement hysteretic loops (as described earlier for the simulated data) using the shear force history estimated from the registered top accelerations multiplied by the mass of the reinforced concrete block at the top, i.e. an ideal SDOF cantilever structure is assumed.

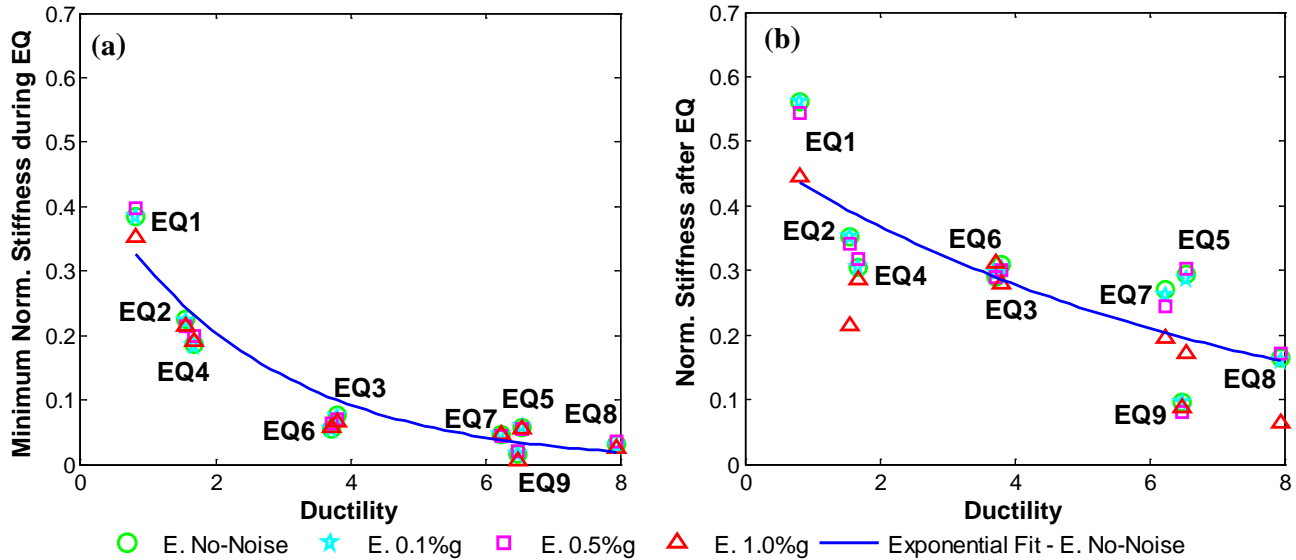


Fig. 7 – Normalized stiffness changes vs. ductility demand using: a) the minimum stiffness reached during the earthquake and, b) the stiffness after the earthquake

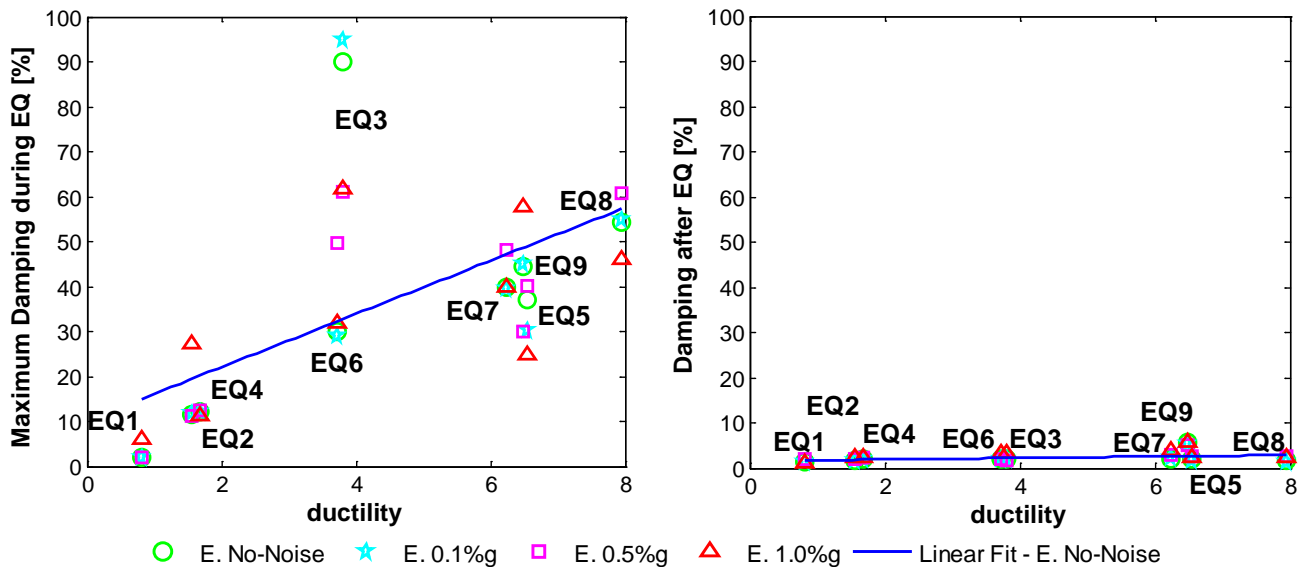


Fig. 8 – Damping ratios vs. ductility demand using: a) the maximum damping ratios reached during the earthquake and, b) the damping ratios after the earthquake

From the results presented in Fig.9 it is seen that the identified displacements are very close to the target values. As it was previously discussed, the residual displacements are not retrieved during the EQs 3, 7 and 8 because of the simplified mathematical model used to represent the column. However, the estimated displacements follow the same trend of the measured response and successfully captured the peak displacements. The identified values of stiffness are consistent with the changes observed in the numerical simulations (Figs. 3(c)-6(c)). Moreover, the initial and final values of the stiffness are close to the estimated stiffness values from

the low amplitude white noise excitations (horizontal lines). The retrieved median damping ratios are consistent with the damping ratios estimated from the experimental data.

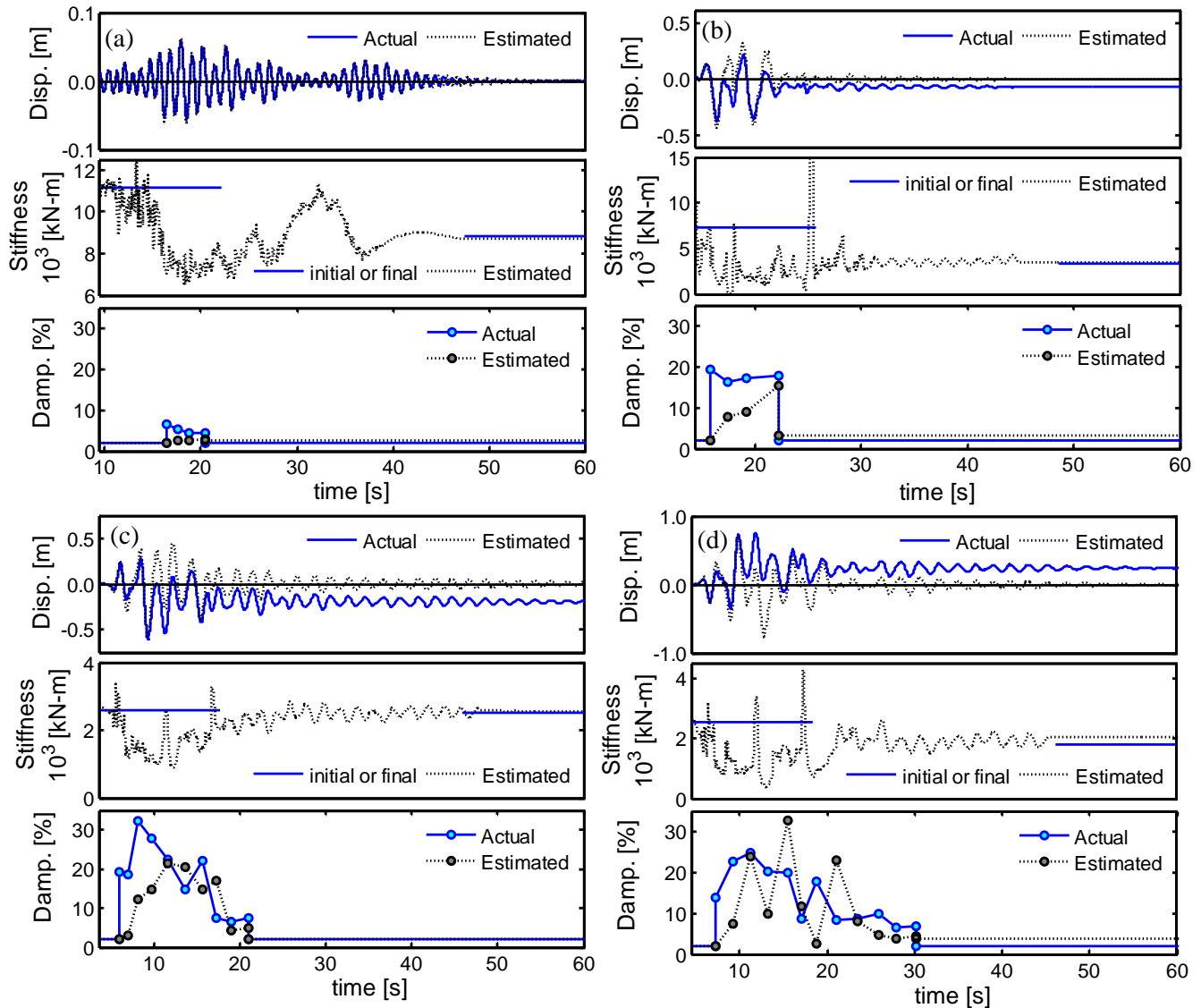


Fig. 9 – Estimated displacement, stiffness and damping ratio time histories (top to bottom) when the column is subjected to: (a) EQ1, (b) EQ3, (c) EQ7 and (d) EQ8.

7. Conclusions

This article presents a UKF based scheme to estimate instantaneous stiffness and damping ratios of RC structures while subjected to earthquake loads. A highlight of the finding is listed next:

- The estimates of the UKF are highly dependent on the definition of the process noise covariance matrix Q . A new approach to define a Q matrix that allows capturing the behavior of stiffness and damping ratios in a wide range of performance level was developed.
- Results using both numerical and experimental data show that damping ratios larger than 30% and normalized stiffness values as low as 5 % can be reached during damaging earthquake loads.
- The maximum values of damping and minimum values of stiffness show a better correlation with the level of ductility reached by the structure than post-event identified values. Specifically, the maximum

values of damping and the minimum values of stiffness depict an approximate linear and exponential correlation with the ductility correspondingly.

8. Acknowledgements

This research is supported by the National Science Foundation Grant No. CMMI-1121146. Any opinions, findings and conclusions or recommendations expressed in this study are those of the writers and do not necessarily reflect the views of the National Science Foundation. The experimental data used in this work was obtained from the NEEShub Project Warehouse, a centralized data repository for sharing and publishing earthquake engineering research data from experimental and numerical studies <https://nees.org/warehouse/project/987/>.

9. References

- [1] Consuegra F, Irfanoglu A (2008): Variation of dynamic properties with displacement in a 3-story reinforced concrete flat plate structure. *14th World Conference on Earthquake Eng.*, 12-17 October, Beijing, China.
- [2] Aguirre DA, Montejo LA (2014): Damping and frequency changes induced by increasing levels of inelastic seismic demand. *Smart Struct. Syst.* **14** (3), 445-468.
- [3] Montejo LA, Gaviria CA, Aguirre DA (2015): Tracking dynamic properties of civil structures while subjected to seismic excitations. *11th Canadian Conference on Earthquake Engineering*, 21-24 July, Victoria, Canada.
- [4] Aguirre DA, Gaviria CA, Montejo LA (2013): Wavelet-Based Damage Detection in Reinforced Concrete Structures Subjected to Seismic Excitations. *J. Earthquake Eng.*, **17** (8) 1103-1125.
- [5] Gaviria, CA, Montejo, LA (2016). Output-only identification of the modal and physical properties of structures using free vibration response. *Earthq. Eng. Eng. Vib.*, **15** (3), 575-589.
- [6] Mariani S, Ghisi A (2007): Unscented Kalman filtering for nonlinear structural dynamics. *J. Nonlinear Dyn.* **49** (1), 131-150.
- [7] Bisht SS, Singh MP (2014): An adaptive unscented Kalman filter for tracking sudden stiffness changes. *Mech. Syst. Signal Proc.* **49** (1-2), 181-195.
- [8] Chaabane M, Majdi M, Hazem N, Mohamed N, and Ahmed BH (2016): Enhanced particle filter for states and parameters estimation in structural health monitoring applications. *Journal of Civil Structural Health Monitoring*. In press.
- [9] Song W, Dyke S (2014): Real-Time Dynamic Model Updating of a Hysteretic Structural System. *J. Struct. Eng.*, **140** (3), 201-214.
- [10] Schoettler MJ, Restrepo JI, Guerrini G, Duck DE, Carrea F (2012): A full-scale, single-column bridge bent tested by shake-table excitation. *Tech. Rep. Center for Civil Engineering Earthquake Research*, Department of Civil Engineering, University of Nevada, Reno, NV.
- [11] Julier SJ, Uhlmann JK (1997): A new extension of the Kalman filter to nonlinear systems. *AeroSense 97 Conference on Photonic Quantum Computing*, 20-25 Apr, Orlando, FL.
- [12] Brown RG, Hwang PY (2012): *Introduction to random signals and applied Kalman filtering*. John Wiley & Sons, 4th edition.
- [13] Priestley M, Calvi G, Kowalsky M (2007): *Displacement based seismic design of structures*. IUSS Press, 1st edition.
- [14] Montejo LA, Kowalsky M, Hassan T (2009): Seismic behavior of flexural dominated reinforced concrete bridge columns at low temperatures. *J. Cold Reg. Eng.* **23** (1), 18-42.
- [15] Aguirre DA, Montejo LA (2015): On the use of numerical models for validation of high frequency based damage detection methodologies. *Structural Monitoring and Maintenance An International Journal* **2** (4), 383-397.